SEARCH FOR POSSIBLE CHARGE NON-CONSERVING DECAY OF ^{139}La INTO ^{139}Ce WITH $LaCl_3$(Ce) SCINTILLATOR

R. BERNABEI, P. BELLI, F. MONTECCHIA, F. NOZZOLI, A. d'ANGELO[1], F. CAPELLA[1], A. INCICCHITTI[1], D. PROSPERI[1], S. CASTELLANO[2], R. CERULLI[2], C.J. DAI[3], V.I. TRETYAK[4]

UDC 539.165

Dipartimento di Fisica, Università di Roma "Tor Vergata" and INFN, Sezione di Roma Tor Vergata
(I-00133 Rome, Italy; e-mail: bernabei@roma2.infn.it),

[1]**Dipartimento di Fisica, Università di Roma "La Sapienza" and INFN, Sezione di Roma**
(I-00185 Rome, Italy),

[2]**INFN, Laboratori Nazionali del Gran Sasso**
(67010 Assergi (AQ), Italy),

[3]**IHEP, Chinese Academy, P.O. Box 918/3**
(100039 Beijing, PR China),

[4]**Institute for Nuclear Research, Nat. Acad. Sci. of Ukraine**
(Kyiv 03680, Ukraine; e-mail: tretyak@kinr.kiev.ua)

A search for the possible charge non-conserving (CNC) decay of ^{139}La into ^{139}Ce has been performed for the first time. For this purpose, a new $LaCl_3$(Ce) crystal scintillator, recently developed, and the low background DAMA/R&D setup have been used to collect the data deep underground at the Gran Sasso National Laboratory of INFN. The limit $\tau_{CNC}(^{139}La\to^{139}Ce) > 1.0\times10^{18}$ yr (90% C.L.) has been obtained for the first time; this limit holds for whatever CNC ^{139}La decay with emission of massless uncharged particles.

1. Introduction

The conservation of the electric charge, which is related to a gauge invariance and masslessness of a photon in accordance with the Weinberg theorem [1], is considered as an absolute law in the standard quantum electrodynamics. Nevertheless, the possibility of CNC phenomena has widely been discussed in the literature (see reviews [2] and references therein) mainly in connection with future unified theories and with the possible existence of extra dimensions [3, 4].

The best up-to-date limits on the CNC processes were established both in searches for electron instabilities (either the electron disappearance or decay into invisible channels: $\tau_e > 2.4\cdot10^{24}$ yr [5], electron disappearance with excitation of low-energy nuclear levels: $\tau_e > 3.7\times10^{24}$ yr [6], and the electron decay into a neutrino and a γ quantum: $\tau_e > 4.6\times10^{26}$ yr [7]; all limits are at 90% C.L.) and in searches for proton instabilities (either disappearance or decay into invisible channels: $\tau_p > 2.1\times10^{29}$ yr [8], $\tau_{pn} > 2.1\times10^{25}$ yr [9], $\tau_{pp} > 5.0\times10^{25}$ yr [10] at 90% C.L.)[1].

[1]It is worth to recall that the DAMA setups have provided along the time several up-to-date limits on the CNC processes, such as: the electron disappearance or decay into invisible channels with DAMA/NaI [5] and with DAMA/LXe [11]; the electron decay into a neutrino and a γ quantum with DAMA/LXe [12]; the electron disappearance with excitation of low-energy nuclear levels in ^{129}Xe with DAMA/LXe [6] and in ^{23}Na and in ^{127}I with DAMA/NaI [13]; the nucleon and di-nucleon decays into invisible channels in ^{129}Xe with DAMA/LXe [14]; the nucleon, di-nucleon, and tri-nucleon decays into invisible channels in ^{136}Xe with DAMA/LXe [15, 16]; the CNC decay $^{136}Xe\to^{136}Cs$ with DAMA/LXe [15].

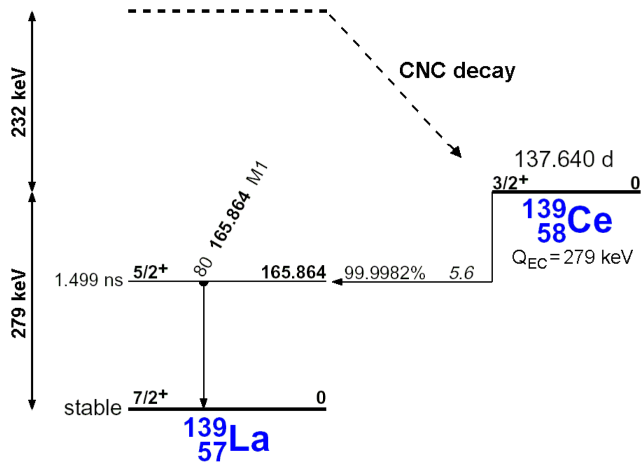

Fig. 1. Scheme of the investigated CNC decay of ^{139}La into ^{139}Ce and of the subsequent EC of ^{139}Ce

An additional approach to investigate the CNC processes is offered by the search for the CNC decay, firstly considered in [17]: if, in a β decay $(A, Z) \to (A, Z+1) + e^- + \overline{\nu}_e$, some massless uncharged particle would be emitted instead of the electron (for example, ν_e or γ or Majoron), an additional 511-keV energy release would occur. Thus, usually forbidden decays to the ground state or to the excited levels of the daughter nuclei would become energetically possible. The presence of the $(A, Z+1)$ isotope or of its daughter products (detected either by chemical methods or through their radioactive decays) in a sample, initially free from them, would indicate the existence of the CNC decay searched for. Up-to-date, only bounds on similar CNC decays are available.

In most of the previous measurements, except, e.g., those in [15, 18], the used technique was traditional to solar neutrino experiments: the chemical separation of the daughter $(A, Z+1)$ element and the search for its radioactive decay with the help of a suitable detector. More recently, it has been proposed [18] instead to exploit a "source = detector" technique in this field, where a parent isotope is not located in a passive target, but it is contained in the used detector itself. The advantages of such an approach are:
(1) the laborious procedure of the chemical separation is avoided;
(2) the events can be processed in a real-time approach, without any loss due to the decay of the $(A, Z+1)$ nuclei from the time of their creation to the time of the chemical separation;
(3) the efficiency to register the decay of the $(A, Z+1)$ nuclei in the used detector will be close to 1;
(4) the analysis of a time evolution of the events' signals can be used to discriminate the effect searched for from other contributions, strongly suppressing the background;
(5) a wider number of nuclei-candidates can be used for the considered CNC decay search (the only request is for the atomic mass of the daughter and parent nuclides, in the ground or excited state: $0 < M(A, Z+1) - M(A, Z) < 511$ keV). Moreover, targets with a quite large mass can, in principle, be used. We firstly exploited this approach in [15] searching for the possible CNC decay of ^{136}Xe into ^{136}Cs.

In the present paper, we describe the first search for the possible CNC decay of ^{139}La into ^{139}Ce, realized by exploiting this new described approach.

The scheme of the process is given in Fig. 1. After the possible ^{139}La CNC decay, the daughter nucleus ^{139}Ce will be created. It transforms back to ^{139}La through the electron capture (EC) with $T_{1/2} = 137.64$ d and $Q_{\rm EC} = 279$ keV [19].

The measurements described here have been performed using a $LaCl_3$(Ce) crystal scintillator in the low background DAMA/R&D setup operating deep underground at the Gran Sasso National Laboratory of INFN.

DAMA/R&D is a multipurpose setup devoted to tests on low background detectors and PMTs and to small scale experiments investigating various processes such as $\beta\beta$ decay modes in ^{40}Ca, ^{46}Ca, ^{48}Ca, ^{106}Cd, ^{130}Ba, ^{136}Ce, ^{138}Ce, ^{142}Ce [20]. The performances and the potentialities of applications of the used $LaCl_3$(Ce) scintillator have been already discussed in [21].

2. Experimental Setup and Measurements

A more detailed description of the used setup has been given elsewhere (see [21]); here we just briefly recall some of its main features.

The used detector is a $LaCl_3$:(8.5±1.0%)Ce (25.4±0.2 mm in diameter and 25.4±0.2 mm in length). It has a density ρ=(3.86±0.01) g/cm^3 [22] corresponding to a mass of (49.7±1.3) g. The crystal is encapsulated in an OFHC copper housing 1 mm in thickness; between copper and the crystal, there are about 2.5 mm of a diffuser. The optical window is made of quartz. The detector is a commercial crystal, and no particular selection of crystal materials has been pursued.

The crystal scintillator has been viewed by a low background photomultiplier (PMT) EMI9265-B53/FL (≃30% quantum efficiency at 380 nm) through a Tetrasil-B light guide (7.6 cm in diameter and 10 cm

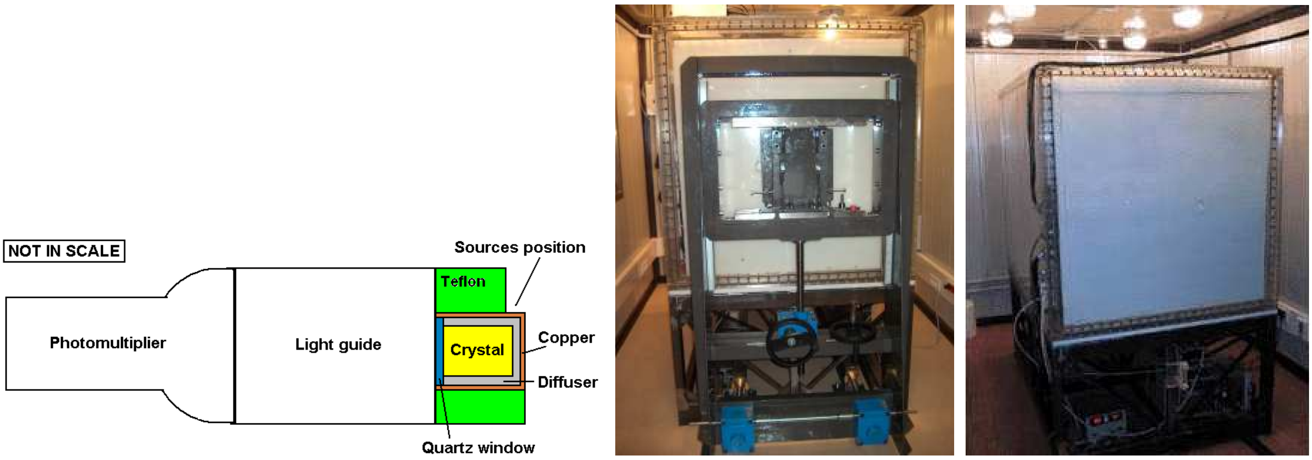

Fig. 2. Schematic view (not in scale) of the $LaCl_3$(Ce) detector inside the inner Cu box of DAMA/R&D (*left*); the authomatic system to close the DAMA/R&D setup (*center*) and the closed shield (*right*)

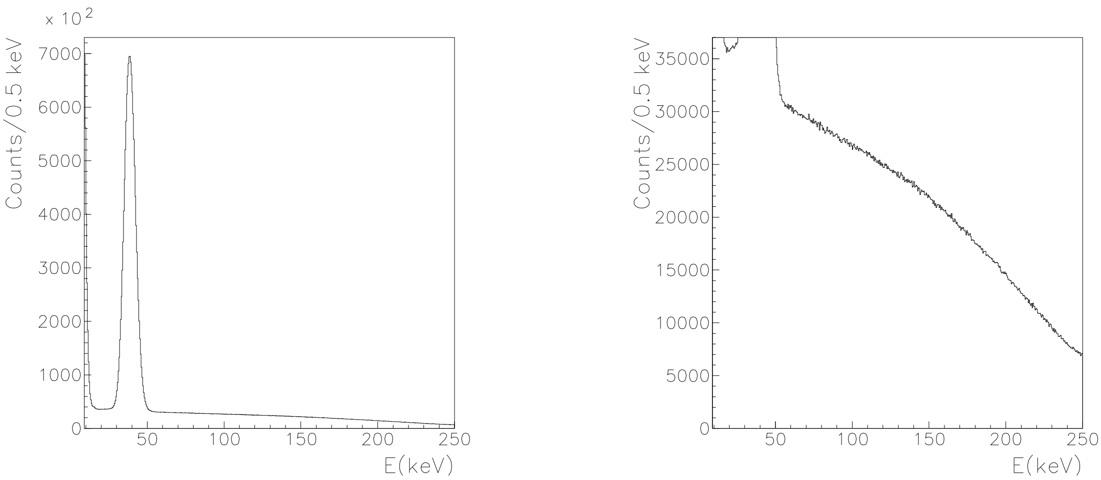

a **b**

Fig. 3. Experimental energy distribution measured deep underground during 493 h by the used $LaCl_3$(Ce) detector in the energy region below 250 keV; the measured counting rate is dominated by the radioactive decays of ^{138}La [21]

long); see Fig. 2. The voltage divider has directly been mounted on the flying leads of the PMT over a teflon disk by using miniaturized SMD capacitors and resistors, soldered by low radioactive lead and special resin.

The detector has been put inside a low-radioactivity sealed copper box filled with low radioactive Cu bricks. The copper box is installed at the center of a low-radioactivity passive shield composed of 10 cm of low radioactive copper, 15 cm of low radioactive lead, $\simeq$1 mm of cadmium, and $\geq$10 cm of polyethylene/paraffin. The inner copper box is flushed with high-purity (HP) nitrogen gas and kept in slightly over-pressure with the respect to the external environment. Also the whole shield is sealed in a plexiglas box and maintained in the HP nitrogen atmosphere (see Fig. 2).

The PMT is connected with a low-noise preamplifier; in the electronic chain, three channels of a charge ADC are acquired (with a 120-ns gate) to collect the information in different energy ranges. Moreover, the signals from the PMT are also recorded by a 160-MSa/s Transient Digitizer over a time window of 3125 ns.

The energy scale is determined with the help of standard gamma sources placed in the position shown in Fig. 2, *left*; the energy resolution has been measured to be: $\frac{\sigma}{E} = 0.004 + \frac{0.59}{\sqrt{E[\text{keV}]}}$ [21].

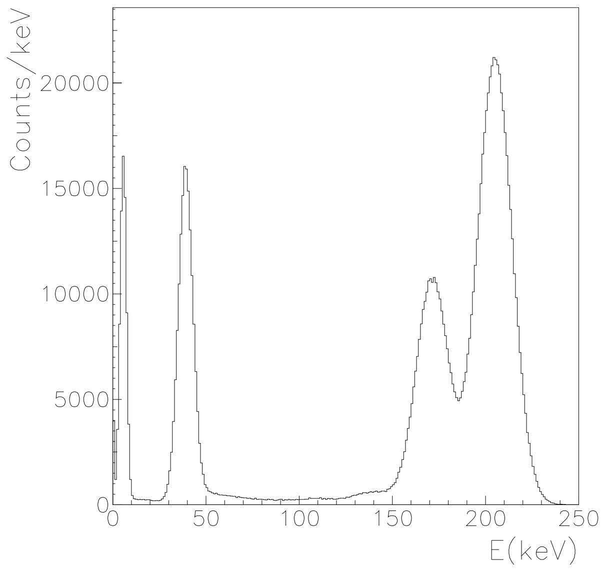

Fig. 4. Expected response function of the $LaCl_3$(Ce) detector for the EC of ^{139}Ce. In the data analysis, presented in the text, the attention has just been paid to the higher energy region

In [21], the whole energy distribution has been given, and the background has been discussed in detail; here instead we focus the attention only on the region of interest for the investigated process. In particular, the experimental energy distribution collected deep underground during 493 h of data taking in the energy region below 250 keV is shown in Fig. 3,*a* and *b*. The measured background is dominated by the internal residual contaminants [21]: the events in this energy region are mainly due to the radioactive decays of ^{138}La (natural abundance: 0.0902%) present in the natural La.

In particular, Fig. 3,*a* shows the peak at $\simeq$38 keV and a part of the peak at 6 keV (shaped by the energy threshold) due to the deexcitation of the shells K and L, respectively, after the EC of ^{138}La in ^{138}Ba (branching ratio: $(66.4 \pm 0.5)\%$ [23]). Moreover, the continuous energy distribution, pointed out in Fig. 3,*b*, is mainly due to the β decay $^{138}\text{La} \rightarrow ^{138}\text{Ce}$ with end-point ~ 250 keV (branching ratio: $(33.6 \pm 0.5)\%$ [23]).

3. Data Analysis and Results

As shown in Fig. 1, the EC process of ^{139}Ce is followed by a γ of $\simeq$166 keV and X rays/Auger electrons. In particular, in the $\sim$70% of events, an electron from shell K ($E_K \simeq 39$ keV) is involved, in the $\sim$23%, an electron from shell L ($E_L \simeq 6$ keV), and, in $\sim$7%, an electron from upper shells.

The expected response function of the $LaCl_3$(Ce) detector for the EC of ^{139}Ce has been simulated with the help of the EGS4 package [24]. The simulated response function is shown in Fig. 4.

The peak at $\simeq$200 keV is due to the sum of the 166-keV γ and X rays/Auger electrons from shell K; the peak at $\simeq$170 keV is due to the sum of the 166-keV γ and X rays/Auger electrons from shell L or upper; moreover, in case of the escape of the 166-keV γ, the X rays/Auger electrons peaks in the low energy region are produced. In particular, in what follows, we consider the higher energy region.

Comparing the experimental energy distribution (given in Fig. 3) with the expected response function (given in Fig. 4), no evidence for the peaks at $\simeq$170 keV and $\simeq$200 keV is found; thus, only a bound on the probability of the investigated effect can be extracted here.

In order to extract the limit on the number of the ^{139}Ce EC decays, the experimental energy distribution in the region 100–240 keV has simultaneously been fitted by the sum of a background model and of the ^{139}Ce EC response function. In that energy region, the experimental energy distribution is mainly due to the β spectrum of ^{138}La decay [21]; thus, following a standard procedure, the number of events N_d – which could be ascribed to the considered decay process – has been calculated by minimizing (with the respect to the P_1 to P_5 and N_d free parameters) the function, $Z^2 = \sum_k \left(F_{P_1\,P_2\,P_3\,P_4\,P_5}(E_k) + N_d M_k - N_k\right)^2 / N_k$, where $F_{P_1\,P_2\,P_3\,P_4\,P_5}(E_k) = f^B_{P_1\,P_2}(E_k) + f^\beta_{P_3\,P_4\,P_5}(E_k)$. The function $f^B_{P_1\,P_2}(E_k) = P_1 + P_2 E_k$ accounts for a linear component of the background, and $f^\beta_{P_3\,P_4\,P_5}(E_k) = \left[\sqrt{E_k(E_k + 2m_ec^2)}(Q_\beta - E_k)^2(E_k + m_ec^2)\right] \quad (P_3 + P_4E_k + P_5E_k^2)$ accounts for the background component arising from the ^{138}La β decay[2].

Moreover, E_k is the mean energy of the k-th energy bin; N_dM_k are the expected counts in the k-th energy bin as evaluated by the Monte Carlo code, while N_k are the measured counts in the given running period and in the k-th energy bin. The Z^2 function has a χ^2 profile; the minimization code uses the well-known MINUIT package, and the MINOS routine is used for the correct evaluation of all the errors of the free parameters of the fit.

[2]A polynomial approximation has been included to take into account the overall effect due to mainly the Fermi function, the spread of the energy resolution, and the high level of forbiddenness of the ^{138}La β decay.

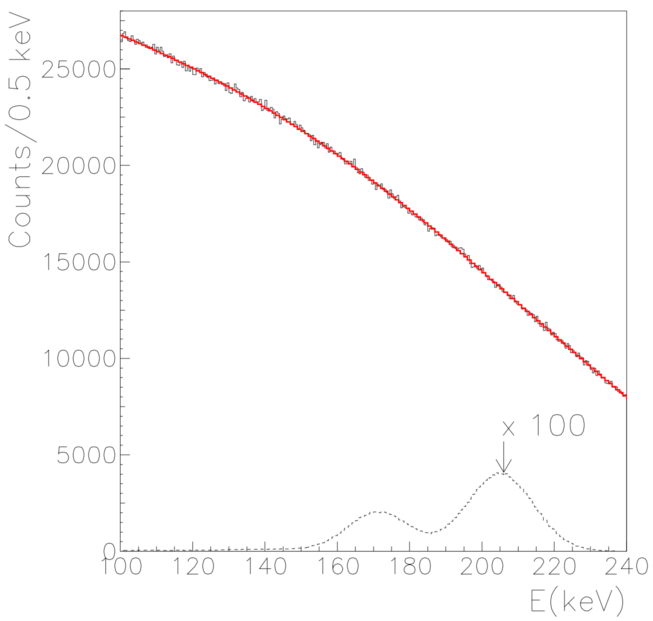

Fig. 5. Experimental energy distribution in the region 100–240 keV (continuous histogram) with the superimposed best-fit curve. The dashed curve is hundred times the energy distribution expected for $\tau_{\rm CNC}$ equal to the 90% C.L. limit obtained following the first procedure described in the text

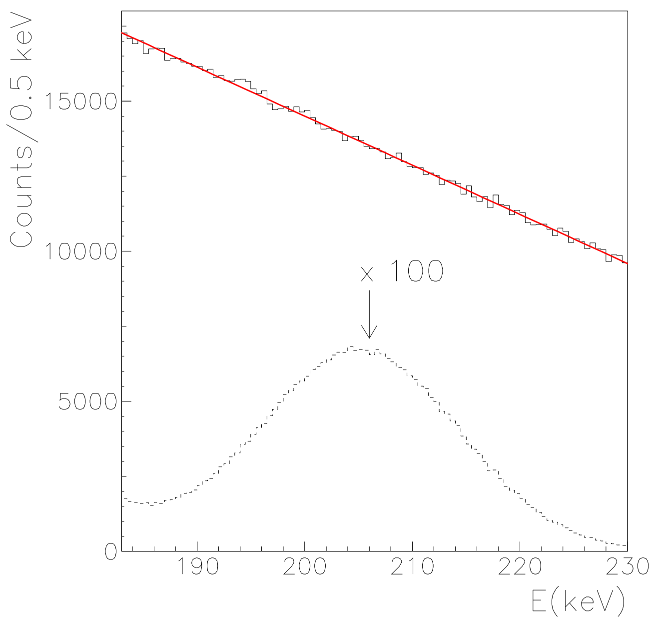

Fig. 6. Experimental energy distribution in the region of the higher energy peak: 183–230 keV (continuous histogram) with the superimposed best-fit curve. The dashed curve is hundred times the energy distribution expected for $\tau_{\rm CNC}$ equal to the 90% C.L. limit obtained by the second approach described in the text

The result of the fit ($\chi^2/d.o.f. \simeq 1$) is $N_d = -3810 \pm 4290$ events; thus, there is no evidence for the effect searched for. According to the Feldman—Cousins procedure [25] recommended by the Particle Data Group [26], the 90% C.L. limit on the number of observed events is $N_d < 3810$ decays.

Then, the corresponding lifetime of the CNC decay of ^{139}La into ^{139}Ce can be calculated by means of the known formula

$$\lim \tau_{\rm CNC} = NT/N_d,$$

where N is the number of ^{139}La nuclei ($N = 1.1 \times 10^{23}$) and T is the time of measurements ($T = 493$ h). Thus, the lifetime limit is

$$\tau_{\rm CNC}(^{139}{\rm La} \rightarrow ^{139}{\rm Ce}) > 1.6 \times 10^{18} \text{ yr at 90\% C.L.}$$

For a direct comparison, the continuous histogram in Fig. 5 represents the experimental data in the region 100—240 keV with the superimposed best-fit curve, while the dashed curve is hundred times the energy distribution expected for $\tau_{\rm CNC}$ equal to the obtained 90% C.L. limit given above.

To test the robustness of the obtained limit, we pursue a second approach focusing the 183–230-keV energy region which is around the $\simeq$200-keV peak expected for the ^{139}Ce EC decay searched for. In this case, the considered background model is simply a straight line: $f^B_{P_1\,P_2}(E_k)$. A standard procedure similar to the one described above has been then followed, obtaining, as a result of the fit, ($\chi^2/d.o.f. \simeq 1$) $N_d = 560 \pm 3530$ events, confirming no evidence for the effect searched for. The 90% C.L. limit on the number of observed events is $N_d < 6370$ for the present approach, and the corresponding lifetime of the CNC decay of ^{139}La into ^{139}Ce is

$$\tau_{\rm CNC}(^{139}{\rm La} \rightarrow ^{139}{\rm Ce}) > 1.0 \times 10^{18} \text{ yr at 90\% C.L.}$$

As is seen, the approaches give the same order of magnitude. To be on the safest side, we will consider, in what follows, the most cautious one. For a direct comparison, the continuous histogram in Fig. 6 represents the experimental data in the region of the higher energy peak: 183—230 keV with the superimposed best-fit curve, while the dashed curve is hundred times the energy distribution expected for $\tau_{\rm CNC}$ equal to the 90% C.L. limit obtained with the second approach.

Limits on lifetime of CNC β decay in various nuclides, τ_{CNC}, established by direct experiments. Corollary bounds just for a single case of CNC decay associated with neutrinos emission, ϵ_ν^2, are also given in the third column (see text)

CNC β decay	τ_{CNC}, yr (C.L.)	ϵ_ν^2	Year [Ref.]
^{87}Rb→^{87m}Sr	$> 1.8 \times 10^{16}$ (68%)	$< 3.3 \times 10^{-17}$	1960 [32]
^{87}Rb→^{87m}Sr	$> 1.9 \times 10^{18}$ (90%)	$< 3.0 \times 10^{-19}$	1979 [33]
^{71}Ga→^{71}Ge	$> 2.3 \times 10^{23}$ (90%)	$< 9.0 \times 10^{-24}$	1980 [34]
^{87}Rb→^{87m}Sr	$> 7.5 \times 10^{19}$ (90%)	$< 7.9 \times 10^{-21}$	1983 [35]
^{113}Cd→^{113m}In	$> 1.4 \times 10^{18}$ (90%)	$< 9.7 \times 10^{-18}$	1983 [36]
^{71}Ga→^{71}Ge	$> 3.5 \times 10^{26}$ (68%)	$< 8.0 \times 10^{-27}$	1996 [37]
^{73}Ge→^{73}As	$> 2.6 \times 10^{23}$ (90%)	$< 1.1 \times 10^{-8}$	2002 [18]
^{136}Xe→^{136}Cs	$> 1.3 \times 10^{23}$ (90%)	$< 1.1 \times 10^{-5}$	2004 [15]
^{115}In→^{115m}Sn	$> 4.1 \times 10^{20}$ (90%)	$< 2.4 \times 10^{-20}$	2005 [38]
^{139}La→^{139}Ce	$> 1.0 \times 10^{18}$ (90%)	$< 4.7 \times 10^{-10}$	This work

The analyzed CNC process can be related to several possible CNC mechanisms with the emission of massless uncharged particles (as Majoron(s), photons, neutrinos, etc.).

In the following, as a corollary result, we will derive — just for a single case of CNC decay associated with the neutrinos emission — a bound on the charge non-conserving admixture in the weak interactions according to the hypothesis of [27]. In fact, under assumption that the weak interactions include a small CNC component of usual form except for a neutrino replacing the electron in the lepton current, $H_{CNC} = \epsilon_\nu H_{usual}$, the ϵ_ν value is related to the τ_{CNC} as follows [27]:

$$\epsilon_\nu^2 = \frac{\tau(n)}{\tau_{CNC}(A,Z)} \frac{W^5(n)}{W^5(A,Z)} \frac{ft_{1/2}(A,Z)}{ft_{1/2}(n)}. \qquad (1)$$

Here, $\tau(n)$ is the neutron lifetime (886.7 s [26]), $W(n)$ is the mass difference between n and p (1293 keV [26]), $W(A,Z)$ is the *nuclear* mass difference between (A,Z) and $(A,Z+1)$ isotopes (232 keV in our case), $ft_{1/2}(n)$ is the n comparative half-life (with the value of $f = 1.692$ [28], we obtain $ft_{1/2}(n) = 1040$ s). The value $ft_{1/2}(A,Z)$ can be estimated from the value of $ft_{1/2}(A,Z+1)$ accounting for the difference in spin between initial and final nuclear states: $ft_{1/2}(A,Z) = ft_{1/2}(A,Z+1)[2J(A,Z)+1]/[2J(A,Z+1)+1]$. In our case, the $ft_{1/2}(A,Z+1)$ for the transition ^{139}Ce→^{139}La(g.s.) was not measured; thus, we use the recommended value for the second-fold forbidden non-unique transitions: $\log ft_{1/2} = 12.5$ [29][3]. With the numbers given above and the most cautious τ_{CNC} limit previously obtained, we get in the present case the restriction: $\epsilon_\nu^2 < 4.7\times10^{-10}$ (90% C.L.) for the considered scenario.

The to-date results on the CNC β decay lifetime in various nuclides are summarized in the Table.

4. Conclusions

In this paper, the data collected deep underground at the Gran Sasso National Laboratory of the INFN have been used to investigate, for the first time, the possible CNC decay of ^{139}La into ^{139}Ce. In spite of the relatively poor radiopurity of the commercial crystal (see, for details, [21]), the most cautious restriction results in

$\tau_{CNC}(^{139}\text{La} \to ^{139}\text{Ce}) > 1.0 \times 10^{18}$ yr at 90% C.L.

This limit holds for whatever CNC ^{139}La decay with the emission of massless uncharged particle (γ, Majoron(s), ν, etc., even some other interesting physics which could appear in future).

1. *Weinberg S.* // Phys. Rev. B. — 1964. — **135**. — P. 1049—1056.
2. *Okun L.B.* // Sov. Phys. Usp. — 1989. — **32**. — P. 543—547; *Okun L.B.* // Comments Nucl. Part. Phys. — 1989. — **19**. — P. 99—116; *Okun L.B.* // Phys. Rev. D. — 1992. — **45**. — P. VI.10—VI.14.
3. *Yndurain F.J.* // Phys. Lett. B. — 1991. — **256**. — P. 15—16; *Arkani-Hamed N., Dimopoulos S., Dvali G.* // Ibid. — 1998. — **429**. — P. 263—272.
4. *Dubovsky S.L., Rubakov V.A., Tinyakov P.G.* // Phys. Rev. D. — 2000. — **62**, 105011. — P. 1—6; *Dubovsky S.L., Rubakov V.A., Tinyakov P.G.* // JHEP. — 2000. — **08**, 041 — P. 1—12.; *Rubakov V.A* // Phys. Uspekhi. — 2001. — **44**. — P. 871—894.
5. *Belli P., Bernabei R., Dai C.J. et al.* // Phys. Lett. B. — 1999. — **460**. — P. 236—241.
6. *Belli P., Bernabei R., Dai C.J. et al.* // Ibid. — 1999. — **465**. — P. 315—322.
7. *Back H.O., Balata M., de Bari A. et al.* // Ibid. — 2002. — **525**. — P. 29—40.
8. *Ahmed S.N., Anthony A.E., Beier E.W. et al.* // Phys. Rev. Lett. — 2004. — **92**, 102004 — P. 1—4.
9. *Tretyak V.I., Denisov V.Yu., Zdesenko Yu.G.* // JETP Lett. — 2004. — **79**. — P. 106—108.
10. *Back H.O., Balata M., de Bari A. et al.* // Phys. Lett. B. — 2003. — **563**. — P. 23—34.
11. *Belli P., Bernabei R., Di Nicolantonio W. et al.* // Astropart. Phys. — 1996. — **5**. — P. 217—219.

[3]The limit $\log ft_{1/2} > 14.5$ is also known from [30], which was based on work [31]. We would like to note here that the to-date $\log ft_{1/2}$ values for the second-fold forbidden beta transitions are known for 27 cases [29]. The central value of the $\log ft_{1/2}$ values is equal to 12.5 with an average deviation of 0.9. For all the investigated cases, the minimum $\log ft_{1/2}$ value is 10.6 and the maximum is 14.15 (only two nuclei have values larger than 14: 14.09 and 14.15). Thus, the only available limit of > 14.5 is quite far from the recommended $\log ft_{1/2}$ value for such transitions, and we decide to use for the present purposes the recommended $\log ft_{1/2}$ value of 12.5.

12. *Belli P., Bernabei R., Dai C.J. et al.* // Phys. Rev. D. — 2000. — **61**, 117301. — P. 1—4.
13. *Belli P., Bernabei R., Dai C.J. et al.* // Phys. Rev. C. — 1999. — **60**, 065501. — P. 1—7.
14. *Bernabei R., Amato M., Belli P. et al.* // Phys. Lett. B. — 2000. — **493**. — P. 12—18.
15. *Bernabei R., Belli P., Cappella F. et al.* // Preprint LNGS/EXP-08/03. — 2003. — P. 1—11; *Bernabei R., Belli P., Cappella F. et al.* Beyond the Desert 2003. — Springer, 2004. — P. 365—374.
16. *Bernabei R., Belli P., Montecchia F. et al.* // Eur. Phys. J. A. — 2006. — **27**, N1.— P.35 —41.
17. *Feinberg G., Goldhaber M.* // Proc. Nat. Acad. Sci. U.S.A. — 1959. — **45**. — P. 1301—1312.
18. *Klimenko A.A., Osetrov S.B., Smolnikov A.A. et al.* // Phys. Lett. B. — 2002. — **535**. — P. 77-84.
19. *Firestone R.B.* Table of Isotopes. — 8-th ed., Wiley, N.Y., 1996 and 1998 CD update.
20. *Bernabei R., Belli P., Incicchitti A. et al.* // Il Nuovo Cimento A. — 1997. — **110**. — P. 189—195; *Belli P., Bernabei R., Incicchitti A. et al.* // Astropart. Phys. — 1999. — **10**. — P. 115—120; *Belli P., Bernabei R., Dai C.J. et al.* // Nucl. Phys. B. — 1999. — **563**. — P. 97—106; *Bernabei R., Belli P., Capella F. et al.* // Nucl. Phys. A. — 2002. — **705**. — P. 29—39; *Belli P., Bernabei R., Cerulli R. et al.* // Nucl. Instr. Meth. A. — 2003. — **498**. — P. 352—361; *Cerulli R., Belli P., Bernabei R. et al.* // Ibid. — 2004. — **525**. — P. 535—543.
21. *Bernabei R., Belli P., Montecchia F. et al.* // Ibid. — 2005. — **555**. — P. 270—281.
22. *Saint Gobain crystals & detectors.* — Private communication.
23. *Tuli J.K.* // Nucl. Data Sheets. — 1995. — **74**. — P. 349—382.
24. *Nelson W.R., Hirayama H., Rogers D.W.O.* // SLAC-Report-265. — Stanford, 1985. — P. 1—205.
25. *Feldman G.J., Cousins R.D.* // Phys. Rev. D. — 1998. — **57**. — P. 3873—3889.
26. *Groom D.E., Aguilar-Benitez M., Amsler C. et al.* // Eur. Phys. J. C. — 2000. — **15**. — P. 1—878.
27. *Bahcall J.N.* // Rev. Mod. Phys. — 1978. — **50**. — P. 881—903; *Bahcall J.N.* Neutrino Astrophysics. — Cambridge University Press, 1989. — P. 359—362.
28. *Dzhelepov B.S., Zyryanova L.N., Suslov Yu.P.* Beta Processes. Functions for Analysis of Beta-spectra and Electron Capture. — Leningrad: Nauka, 1972 (in Russian).
29. *Singh B., Rodriguez J.L., Wong S.S.M. et al.* // Nucl. Data Sheets. — 1998. — **84**. — P. 487—563.
30. *Burrows T.W.* // Ibid. — 2001. — **92**. — P. 623—782.
31. *Minova M., Inoue Y., Asanuma T. et al.* // Phys. Rev. Lett. — 1993. — **71**. — P. 4120—4123.
32. *Sunyar A.W., Goldhaber M.* // Phys. Rev. — 1960. — **120**. — P. 871—873.
33. *Norman E.B., Seamster A.G.* // Phys. Rev. Lett. — 1979. — **43**. — P. 1226—1229.
34. *Barabanov I.R., Veretenkin E.P., Gavrin V.N. et al.* // JETP Lett. — 1980. — **32**. — P. 359—362.
35. *Vaidya S.C., Roy A., Ephraim D.C. et al.* // Phys. Rev. D. — 1983. — **27**. — P. 486—492.
36. *Roy A., Vaidya S.C., Ephraim D.C. et al.* // Ibid. — 1983. — **28**. — P. 1770—1772.
37. *Norman E.B., Bahcall J.N., Goldhaber M.* // Ibid. — 1996. — **53**. — P. 4086—4088.
38. *Cattadori C.M., De Deo M., Laubenstein M. et al.* // Nucl. Phys. A. — 2005. — **748**. — P. 333—347.

Received 17.04.06

ПОШУК МОЖЛИВОГО РОЗПАДУ ^{139}La В ^{139}Ce ІЗ НЕЗБЕРЕЖЕННЯМ ЕЛЕКТРИЧНОГО ЗАРЯДУ ЗА ДОПОМОГОЮ СЦИНТИЛЯТОРА $LaCl_3$(Ce)

Р. Бернабей, П. Беллі, Ф. Монтеккі, Ф. Ноццолі, А. д'Анджело, Ф. Капелла, А. Інчікітті, Д. Проспері, С. Кастеллано, Р. Черуллі, С.Й. Дай, В.І. Третяк

Р е з ю м е

В перший раз виконано пошук можливого розпаду ^{139}La в ^{139}Ce з порущенням закону збереження електричного заряду (ЗЗЕЗ). В досліді був використаний нещодавно розроблений кристалічний сцинтилятор $LaCl_3$(Ce) та низькофонова установка DAMA/R&D. Експериментальні дані накопичені глибоко під землею в Національній лабораторії Гран Сассо (Італія). Одержане вперше обмеження $\tau_{\rm CNC}(^{139}{\rm La}\rightarrow^{139}{\rm Ce}) > 1,0 \cdot 10^{18}$ років (90% C.L.) є правильним для будь-якого процесу з порушенням ЗЗЕЗ з випромінюванням безмасової нейтральної частинки.